Repression of flowering under a noninductive photoperiod by the *HDA9-AGL19-FT* module in Arabidopsis

Min-Jeong Kang[1], Hong-Shi Jin[1], Yoo-Sun Noh[1,2] and Bosl Noh[3]

[1]School of Biological Sciences, Seoul National University, Seoul 151-747, Korea; [2]Plant Genomics and Breeding Institute, Seoul National University, Seoul 151-742, Korea; [3]Research Institute of Basic Sciences, Seoul National University, Seoul 151-747, Korea

Authors for correspondence:
Bosl Noh
Tel: +82 2 871 6675
Email: bnoh2003@gmail.com

Yoo-Sun Noh
Tel: +82 2 880 6674
Email: ysnoh@snu.ac.kr

Received: *27 August 2014*
Accepted: *8 October 2014*

New Phytologist (2015) **206:** 281–294
doi: 10.1111/nph.13161

Key words: AGAMOUS-LIKE 19 (AGL19), *Arabidopsis thaliana*, chromatin, flowering, HDA9, histone deacetylation.

Summary

- Posttranslational acetylation of histones is reversibly regulated by histone deacetylases (HDACs). Despite the evident significance of HDACs in Arabidopsis development, the biological roles and underlying molecular mechanisms of many HDACs are yet to be elucidated.
- By a reverse-genetic approach, we isolated an *hda9* mutant and performed phenotypic analyses on it. In order to address the role of HDA9 in flowering, genetic, molecular, and biochemical approaches were employed.
- *hda9* flowered early under noninductive short-day (SD) conditions and had increased expression of the floral integrator *FLOWERING LOCUS T* (*FT*) and the floral activator *AGAMOUS-LIKE 19* (*AGL19*) compared with the wild-type. The *hda9* mutation increased histone acetylation and RNA polymerase II occupancy at *AGL19* but not at *FT* during active transcription, and the HDA9 protein directly targeted *AGL19*. *AGL19* expression was higher under SD than under inductive long-day (LD) conditions, and an *AGL19* overexpression caused a strong up-regulation of *FT*. A genetic analysis showed that an *agl19* mutation is epistatic to the *hda9* mutation, masking both the early flowering and the increased *FT* expression of *hda9*.
- Taken together, our data indicate that HDA9 prevents precocious flowering under SD conditions by curbing the hyperactivation of *AGL19*, an upstream activator of *FT*, through resetting the local chromatin environment.

Introduction

Histone acetylation has been implicated in transcriptional activation. The addition of acetyl groups on lysine residues at the histone N-terminal tails by histone acetyltransferases (HATs) decreases the affinity of DNA to histones by increasing negative charges on histones, thereby relaxing the chromatin structure to be more accessible to transcription factors. The histone-tail acetylation also creates binding surfaces for other chromatin modifiers or transcription cofactors positively regulating transcription. Histone deacetylases (HDACs) remove acetyl groups from histone lysine residues, which results in the opposite effects to HATs on chromatin structure and transcription. In fact, HDACs have been found in various types of transcription repressor complexes in yeasts and higher eukaryotes (Cunliffe, 2008; Yang & Seto, 2008). Interestingly, genome-wide association studies on yeast and in humans have shown the presence of HDACs together with HATs in active as well as in inactive genes (Kurdistani *et al.*, 2002; Wang *et al.*, 2009b), suggesting a role of HDACs in controlling transcription that is beyond the traditional paradigm.

Arabidopsis has 12 putative HDACs belonging to the RPD3/HDA1 superfamily that is divided into four subgroups, namely class I through III and an outlier group (Pandey *et al.*, 2002). Genetic or pharmacological ablation of the HDAC function has shown that HDACs play diverse and important roles in many aspects of development and physiology in Arabidopsis. Antisense or T-DNA insertional knockout mutants of *HDA19*, a class I *HDAC*, show multiple defects in growth and development and altered responses to exogenous stimuli, such as light and pathogens, accompanied by deregulation of genes (Tian *et al.*, 2003; Zhou *et al.*, 2005; Benhamed *et al.*, 2006; Long *et al.*, 2006; Kim *et al.*, 2008; Tanaka *et al.*, 2008; Choi *et al.*, 2012), reflecting the role of HDA19 as a global repressor (Tian *et al.*, 2005). HDA6, the closest homolog of HDA19, plays key roles in the silencing of transgenes, transposable elements, and rRNA genes in association with RNA-directed DNA methylation (RdDM; Aufsatz *et al.*, 2002; Probst *et al.*, 2004; Earley *et al.*, 2010) or RdDM-independent DNA methylation (To *et al.*, 2011; Liu *et al.*, 2012). Studies using *hda6* mutants have revealed that HDA6 has roles in flowering (Wu *et al.*, 2008; Yu *et al.*, 2011), embryonic-to-postembryonic transition (Tanaka *et al.*, 2008), and senescence (Wu *et al.*, 2008). Pharmacological studies employing trichostatin A (TSA), an inhibitor of the RPD3/HDA1 family of HDACs, have also revealed the importance of HDACs in directing the expression of root epidermal cell-patterning genes (Xu *et al.*, 2005) and in controlling the

rhythmic expression of the circadian clock gene, *TOC1* (Perales & Màs, 2007).

Flowering is controlled by environmental cues, such as photoperiod and temperature, and by developmental signals. In facultative long-day plants including Arabidopsis, inductive long-day (LD) conditions promote rapid flowering, whereas noninductive short-day (SD) conditions repress the floral promotion activity and thus results in delayed flowering (Koornneef *et al.*, 1998). There have been extensive studies on the signaling and mechanism of LD-induced floral promotion (Turck *et al.*, 2008; reviewed in Amasino, 2010); however, the signaling and mechanistic detail of floral repression and default flowering under SD conditions are poorly understood. Gibberellic acid (GA) is known to allow default flowering under SD conditions through activation of *SUPPRESSOR OF OVEREXPRESSION OF CONSTANS 1* (*SOC1*) and *LEAFY* (*LFY*), two of the downstream floral activators (Blázquez & Weigel, 2000; Moon *et al.*, 2003). VIN3-LIKE 1 (VIL1) and VIL2 have been reported to repress *FLOWERING LOCUS M* (*FLM*) and *MADS AFFECTING FLOWERING 5* (*MAF5*), two of the *FLOWERING LOCUS C* (*FLC*)-clade floral repressors, respectively under SD conditions, leading to the promotion of floral transition (Sung *et al.*, 2006; Kim & Sung, 2010). Recently, the microRNA156 (miR156)-*SQUAMOSA PROMOTER BINDING PROTEIN LIKEs* (*SPLs*) regulatory module for vegetative phase transition has also been shown to play an important role in age-dependent flowering, especially under noninductive SD conditions (Wang *et al.*, 2009a).

Although there is evidence indicating the significance of HDACs in the development and physiology of Arabidopsis, the biological roles and underlying molecular mechanisms of many HDACs have not yet been studied. Here, we report on the *in vivo* roles of HDA9, a member of the RPD3/HDA1 family class I HDACs. Loss of *HDA9* affects the development of several organs and caused early flowering under SD conditions. Recently, a SD-specific early flowering of *hda9* mutants with increased *AGAMOUS-LIKE 19* (*AGL19*) expression and histone acetylation at the *AGL19* locus was reported (Kim *et al.*, 2013). However, several important questions, including whether *AGL19* is a direct target of HDA9, whether the increased expression of *AGL19* is a direct cause of the early flowering of *hda9*, and how the loss of HDA9 activity results in SD-specific early flowering, remain unanswered. Moreover, the pathway for which *AGL19* acts as a floral activator has not been elucidated. We demonstrate that HDA9 prevents precocious flowering under SD conditions and during vernalization by directly targeting *AGL19* and repressing its expression during active transcription through histone deacetylation. Derepression of *AGL19* caused by the *hda9* mutation in turn induces the expression of *FLOWERING LOCUS T* (*FT*), which results in early flowering. We also show that *AGL19* expression is up-regulated by a SD photoperiod as well as by vernalization (Schönrock *et al.*, 2006). These results indicate that the role of HDA9 in preventing the overstimulation of *AGL19* transcription by the inductive signals, together with the photoperiod-dependent expression of *AGL19* form the basis of the SD-specific early flowering of *hda9*. Our results suggest that the biochemical role of HDA9 might be to reset histone acetylation levels during active transcription to attain proper transcription activity and controlled gene expression.

Materials and Methods

Plant materials and growth conditions

Arabidopsis thaliana (L.) Heynh Columbia-0 (Col-0) was employed as the wild-type (wt) and also as the genetic background of the transgenic plants and mutants used in this study. The following T-DNA insertion mutants were obtained from the SALK collection (http://signal.salk.edu/) and genotyped by using gene-specific primers (Supporting Information, Table S1): *hda9-1*, SALK_007123; *maf4*, SALK_028506; *maf5-1*, CS876411; and *maf5-2*, SALK_054770. The following mutants and transgenic plants were previously described as written in the text: *flc-3*, *fld-3*, *ld-1*, *FRI*, *hac1-1*, *ref6-3*; *co-101*, *ft-10*, *gi-2*, *agl19-1* and *FT::GUS* plants. All the plants were grown at 22°C under 100 μmol m^{-2} s^{-1} of cool white fluorescent light with a photoperiod of either 16 : 8 h, light: dark (LD condition for this study) or 8 : 16 h, light : dark (SD condition for this study).

Histochemical β-glucuronidase (GUS) assay

For *HDA9:GUS*, a 3.9 kb genomic fragment of *HDA9* containing a 0.9 kb promoter and the entire coding region was generated by PCR using HDA9-GUS-F and HDA9-GUS-R as primers (Table S2). After restriction digestion with *Xho*I-*Sma*I, the PCR product was ligated to the *Sal*I-*Sma*I digested pPZP211G (Noh *et al.*, 2001). *HDA9:GUS* was introduced into the wt by the floral dip method (Clough & Bent, 1998) via *Agrobacterium tumefaciens* strain ABI, and transformants were selected on MS media containing 50 μg ml^{-1} kanamycin. Histochemical GUS staining was performed as previously described (Noh *et al.*, 2004). The GUS expression patterns in Fig. 2(b,c) were observed using a light microscope (Carl Zeiss Axioskop 40). *FT::GUS* from the wt was introgressed into *hda9-1* through crossing, and the *hda9-1* mutants carrying *FT::GUS* (+/+) were selected. FT::GUS expression patterns in the wt and *hda9-1* were then compared.

Subcellular localization study

Nuclear fractionation was performed as previously described (Kinkema *et al.*, 2000). Protein samples were quantified using a protein assay kit (Bio-Rad), subjected to sodium dodecyl sulfate polyacrylamide gel electrophoresis (SDS-PAGE), and transferred to nitrocellulose membranes (Millipore). For the detection of proteins, α-HA (Abcam ab9110), α-H3 (Abcam ab1791), and α-tubulin (Sigma-Aldrich T9026) were used at 1 : 3000, 1 : 10 000, and 1 : 4000, respectively.

HDA9 complementation construct and HDA9:HA

For the complementation construct (*HDA9g*), a 3.9 kb genomic fragment was amplified by PCR using HDA9-GUS-F and

HDA9G-R (Table S2) as primers and cloned into the pPZP221-rbcsT, which contains the transcriptional terminator of Arabidopsis *rbcS*. For the construction of *HDA9:HA*, a 3.9 kb *HDA9* genomic fragment amplified using HDA9 gateway-F and HDA9 gateway-R as primers (Table S2) was cloned into the pENTR/SD/D-TOPO entry vector (Invitrogen) and then integrated into the pEarleyGate 301 destination vector (Earley *et al.*, 2006) through recombination. The complementation construct and *HDA9:HA* were introduced into *hda9-1* as described for *HDA9:GUS*, and transformants were selected on MS media containing 100 μg ml^{-1} gentamycin (Sigma-Aldrich) or 25 μg ml^{-1} glufosinate ammonium (Sigma-Aldrich), respectively.

Flowering time analysis

Flowering times were measured as the means ± SD of the number of rosette and cauline leaves produced from the primary meristems at bolting. At least 15 plants were scored for each genotype and treatment. For vernalization treatment, plants were grown for 14 d (d) under SD conditions and vernalized at 4°C under SD conditions for 30 d. Vernalized samples were harvested immediately after the cold treatment.

RT-PCR and RT-qPCR analyses

Total RNA was isolated from plant tissues using TRI Reagent (Sigma-Aldrich) according to the manufacturer's instructions. Four micrograms of total RNA were reverse-transcribed using MMLV Reverse Transcriptase (Fermentas, Seoul, Korea) and the resulting first strand was used as a template for semiquantitative PCR or quantitative real-time PCR (qPCR). The sequences of primers used for reverse transcription followed by PCR (RT-PCR) or qPCR (RT-qPCR) are provided in Table S3 or Table S4, respectively. qPCR was performed in 96-well blocks using an Applied Biosystems 7300 real-time PCR system (http://www.appliedbiosystems.com/) and SYBR Green I master mix (Kappa Biosystems). Absolute quantification was performed by generating standard curves using serial dilutions of a mixture of all cDNA samples to be analyzed. Normalization was to *Ubiquitin 10* (*UBQ10*). All the RT-qPCR results were presented as means ± SE of three biological replicates performed in triplicate.

Chromatin immunoprecipitation (ChIP) assay

Chromatin immunoprecipitation was performed as previously described (Han *et al.*, 2007; Kaufmann *et al.*, 2010). Antibodies used for ChIP were α-H3Ac (Millipore) 06-599, α-H3 (Abcam ab1791), α-RNA PolII (Covance MMS-126R), and α-HA (Abcam ab9110). The α-H3Ac recognizes acetylated lysine 9 and 14 of H3, and the α-RNA PolII recognizes both the initiating and elongating forms of PolII. The amount of immunoprecipitated chromatin was determined by qPCR (ChIP-qPCR) using primer pairs listed in Table S5, and the relative amounts of amplified products were evaluated according to the $2^{-\Delta\Delta CT}$ method (Livak & Schmittgen, 2001).

Results

Isolation of an *hda9* mutant

The amino acid sequence alignment of HDA9 (At3g44680) and other Arabidopsis Rpd3/HDA1 class I HDACs (HDA6, HDA7, and HDA19) showed that the HDAC domain of HDA9 is highly similar to that of other HDACs, but its C-terminal region is quite divergent and varies in length compared with that of others (Fig. S1a). Interestingly, the C-terminal region of HDA9 (277–426) is nearly identical to the entire regions of HDA10 and HDA17, which belong to the outlier group (Fig. S1b; Pandey *et al.*, 2002; Hollender & Liu, 2008). However, HDA10 and HDA17 possess partial HDAC domains and are thus unlikely to be functionally redundant with HDA9 (Fig. S1b). These structural features suggest that HDA9 might possess a unique role in Arabidopsis.

To address the biological role of HDA9 and determine if it is distinct from the roles of the well-characterized HDA6 and HDA19, we first isolated a mutant carrying a T-DNA insertion in the fourth exon of *HDA9* from the SALK collection and named it *hda9-1* (Fig. 1a). This mutant allele was also reported by Kim *et al.* (2013). RT-PCR analyses showed that the full-length *HDA9* transcript is not expressed at a detectable level, although a truncated transcript upstream of the T-DNA insertion site in *hda9-1* is expressed at a reduced level (Fig. 1b). Thus, *hda9-1* is believed to be a null allele.

The *hda9-1* mutants showed a normal morphology in most organs in contrast to *hda19* mutants, which display severely distorted morphological phenotypes in many organs (Tian & Chen, 2001; Tian *et al.*, 2003; Long *et al.*, 2006). Nonetheless, subtle morphological differences between wt and *hda9-1* were observed in a few organs. At the fully developed stage, *hda9-1* flowers did not open as fully as wt flowers, and the petals and sepals were less tightly attached to the receptacles in *hda9-1* than in wt (Fig. 1c). In addition, the tips of the *hda9-1* siliques were wide and blunt, whereas those of the wt siliques were tapered and acute (Fig. 1d). The *hda9-1* silique phenotype was similar to that of *erecta* (*er*) mutants (Torii *et al.*, 1996). However, unlike *er* mutation, the *hda9-1* mutation did not affect silique length (Figs 1, S2a). In addition, the size of adult *hda9-1*, especially when grown in SD, was smaller than the wt, mainly because of less elongated petioles and leaves (Figs 1e,f, S2b). All of these *hda9-1* phenotypes were restored to wt phenotypes when a genomic copy of *HDA9* was introduced into the *hda9* mutant plants (Fig. 1c,d,f), demonstrating that these phenotypes are indeed caused by the loss of *HDA9* function. Because the *hda9-1* phenotypes described here have not been reported for either *hda6* or *hda19*, it is likely that HDA9 has a distinct *in planta* role or it is also possible that these phenotypes have not yet been carefully analyzed in *hda6* or *hda19*.

Spatial expression pattern and nuclear localization of HDA9

Because the expression pattern of *HDA9* has not been reported previously, we generated transgenic plants harboring the native promoter and genomic coding region of *HDA9* translationally

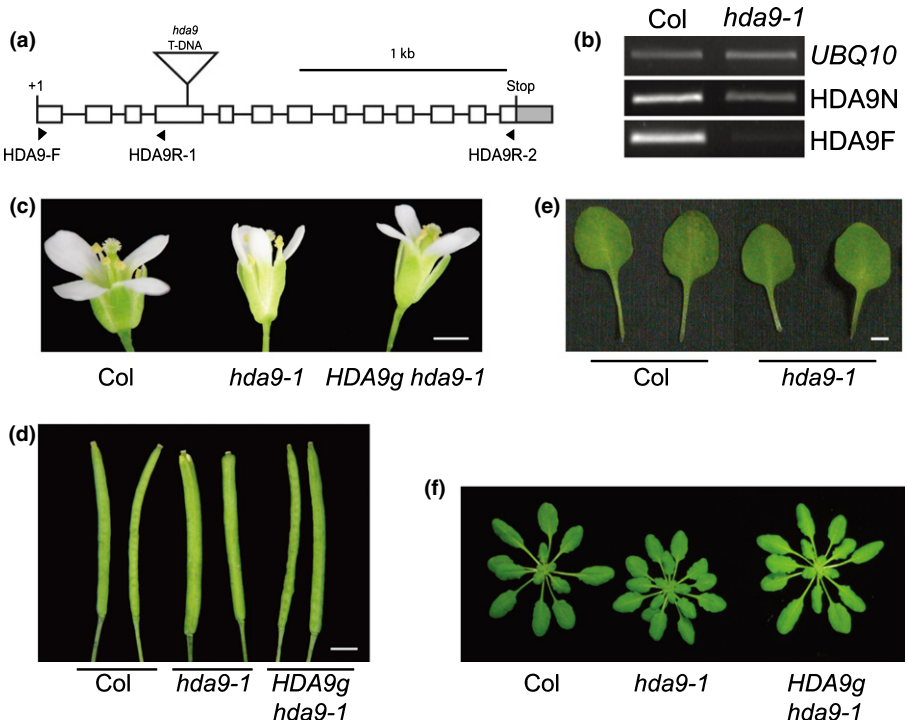

Fig. 1 Phenotype of *Arabidopsis thaliana hda9-1* mutant. (a) Schematic illustration of the gene structure of *HDA9* and a T-DNA insertion in *hda9-1*. Exons and the 3′ untranslated region (UTR) are represented with white boxes and a gray box, respectively. Introns are indicated as solid lines. +1, the transcription start site; triangle, the T-DNA insertion position in *hda9-1*; arrows, the primers used for reverse transcription polymerase chain reaction (RT-PCR) in (b). (b) RT-PCR analysis of a 5′ (HDA9N) and the full-length (HDA9F) *HDA9* transcript expression in wild-type (wt, Col) and *hda9-1* plants. HDA9-F/HDA9-R1 and HDA9-F/HDA9-R2 primer pairs (a; Table S3) were used for HDA9N and HDA9F, respectively. *UBQ10* was used as an expression control. (c, d) Flower (c) and silique (d) phenotype of wt, *hda9-1*, and *hda9-1* transformed with a genomic copy of *HDA9* (*HDA9g hda9-1*). Bars, 1 mm. (e) Representative fifth and sixth rosette leaves with petioles of wt and *hda9-1* plants grown for 45 d under short-day conditions. Bars, 5 mm. (f) Rosette development in wt, *hda9-1* and *HDA9g hda9-1* plants. Shown are plants grown for 45 d in SD.

fused to *GUS* (*HDA9:GUS*), and performed histochemical analyses to study the spatial expression pattern of *HDA9*. GUS staining was observed in the cotyledons, hypocotyls, and roots of the seedlings (Fig. 2a). The shoot apexes, leaf primordial, and root tips were the organs most strongly stained (Fig. 2b,c). In older developmental stages, GUS staining was detected in the entire rosette leaves, including the trichomes and petioles (Fig. 2d), floral organs, such as the stigmas, anthers, filaments, and pollens, and the siliques (Fig. 2e,f). The nearly ubiquitous spatial expression pattern of *HDA9* studied with the *HDA9:GUS* plants was confirmed by RT-qPCR using RNAs obtained from various tissues (Fig. 2g) and by analysis of the expression profile of *HDA9* exploiting publicly available microarray datasets (Fig. S3).

As shown in Fig. 2(c), HDA9:GUS expression was dispersed but not restricted to any particular subcellular compartment. However, it was not clear whether this subcellular GUS-staining pattern reflects the real subcellular localization of the HDA9 protein, because *HDA9:GUS* was not able to complement *hda9-1*. Therefore, we generated transgenic *hda9-1* plants expressing the HDA9 protein with a C-terminal HA tag (HDA9:HA) from the native *HDA9* promoter. Unlike *HDA9:GUS*, *HDA9:HA* was able to fully rescue the *hda9-1* mutant phenotypes (Fig. S4a–d), indicating that HDA9:HA is functionally equivalent to HDA9. To determine the subcellular localization of HDA9:HA, nonnuclear and nuclear proteins were fractionated from the *HDA9:HA hda9-1* plants and used for immunoblot analysis using an anti-HA antibody. A *c.* 55 kDa protein corresponding to HDA9:HA was detected in the nuclear but not in the nonnuclear fraction (Fig. 2h). Thus, HDA9 seems to be localized predominantly in the nuclei, like HDA6 and HDA19 (Earley *et al.*, 2006; Fong *et al.*, 2006; Long *et al.*, 2006; Wu *et al.*, 2008).

The *hda9-1* mutation causes early flowering under SD conditions

The *hda9-1* mutants displayed another remarkable phenotype: an early flowering under noninductive SD conditions, as evidenced by a smaller number of rosette leaves at the onset of flowering (Fig. 3a,b) without a change in leaf initiation rate (Fig. S4e). The early-flowering phenotype of *hda9-1* was rescued by the introduction of a genomic *HDA9* fragment (*HDA9g*; Fig. 3a, b) and by *HDA9:HA* (Fig. S4b,d). However, the early-flowering phenotype of *hda9-1* was not obvious under inductive LD conditions (Figs 3c,d, S4a,c).

We then analyzed the genetic interactions between *hda9-1* and mutations in the autonomous pathway, the photoperiod pathway, and the floral integrator group. The *hda9-1* mutation caused partial suppression of the late-flowering phenotypes of the

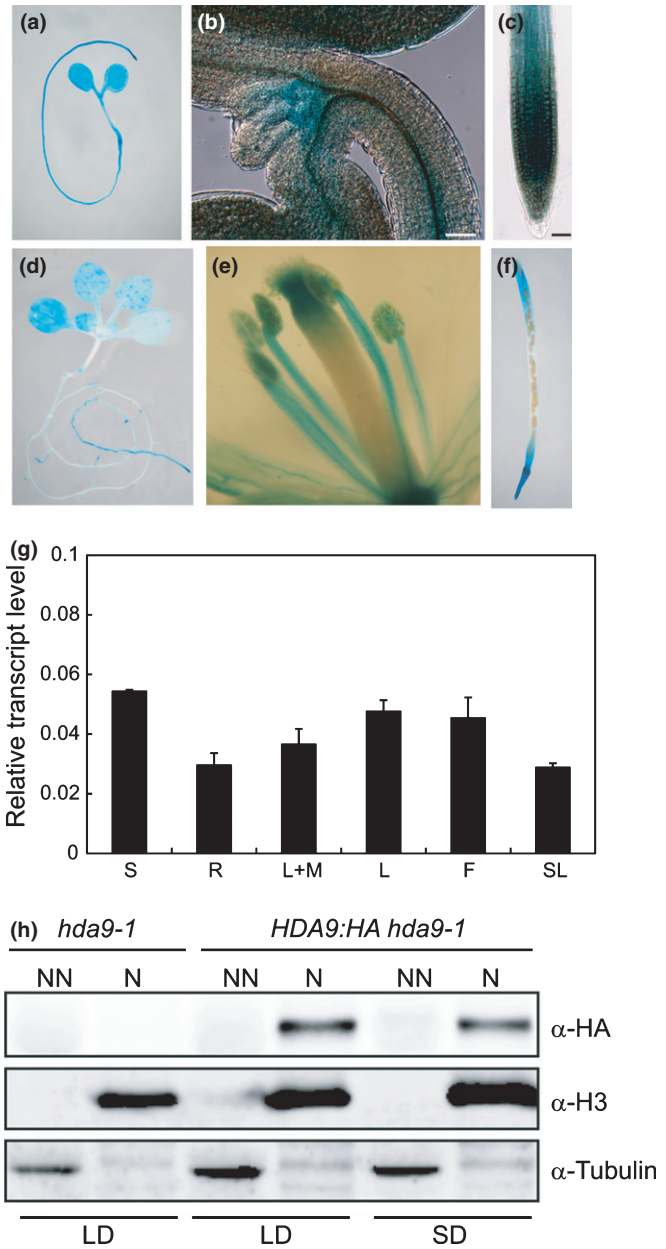

Fig. 2 Expression pattern of *Arabidopsis thaliana HDA9*. (a–f) Histochemical β-glucuronidase (GUS) staining of *HDA9:GUS*-containing transgenic Arabidopsis. (a) Four-day-old seedling grown under short-day (SD) conditions. (b) Magnified shoot apex of the seedling shown in (a). (c) Primary root tip of 6-d-old seedling grown in SD. Bars (b, c): 50 μm. (d) Sixteen-day-old whole seedling grown under SD conditions. (e, f) Open flower (e) and silique (f) of long day (LD)-grown plant. (g) mRNA expression of *HDA9* in various tissues as studied by quantitative real-time reverse transcription polymerase chain reaction (RT-qPCR). RNA was isolated from 10-d-old seedlings (S), roots (R), entire shoots including the shoot apical meristems (L+M), rosette leaves (L), flowers (F), and siliques (SL). *UBQ10* was used as an expression control. Values are the means ± SD of three technical replicates. (h) Nuclear localization of HDA9. Nuclear (N) and nonnuclear (NN) proteins were extracted from *hda9-1* and *HDA9:HA*-containing *hda9-1* transgenic seedlings grown for 10 d under LD or 14 d under SD conditions and subjected to immunoblot analysis with anti-HA antibody. Histone H3 and tubulin were detected as nuclear and nonnuclear protein controls, respectively.

autonomous-pathway mutants *hac1-1* (Han *et al.*, 2007), *relative of early flowering 6-3* (*ref6-3*; Noh *et al.*, 2004), *flowering locus d-3* (*fld-3*; He *et al.*, 2003), *luminidependens-1* (*ld-1*; Lee *et al.*, 1994), and *FRIGIDA* (*FRI*; Koornneef *et al.*, 1994; Lee *et al.*, 1994)-containing Col under LD conditions (Fig. 3e) and, to a greater extent, under SD conditions (Fig. 3f). The late-flowering phenotypes of the photoperiod-pathway mutants were also suppressed by *hda9-1*, but not as effectively as those of the autonomous-pathway mutants: the *gigantea-2* (*gi-2*; Park *et al.*, 1999) *hda9-1* and *constans-101* (*co-101*; Takada & Goto, 2003) *hda9-1* double mutants flowered slightly earlier than the *gi-2* and *co-101* single mutants, respectively (Fig. 3g,h). Notably, the *hda9-1* mutation was not capable of accelerating the floral transition of a floral integrator mutant, *flowering locus t-10* (*ft-10*; Yoo *et al.*, 2005), under both LD and SD conditions (Fig. 3g,h), indicating that *FT* acts downstream of *HDA9*. These results indicate that *HDA9* negatively regulates flowering in parallel with the autonomous and photoperiod pathways and acts upstream of *FT*.

The day length-dependent effect of the *hda9-1* mutation on flowering (Fig. 3a–d) raised a possibility of day length-dependent *HDA9* expression or nuclear-cytoplasmic shuttling of HDA9 protein as the mammal class II HDACs (Grozinger & Schreiber, 2000; Verdel *et al.*, 2000). However, HDA9:HA protein was accumulated to comparable levels in both LD- and SD-grown plants and predominantly localized to nuclei in both photoperiodic conditions (Fig. 2h), excluding those possibilities.

Loss of *HDA9* affects the expression of *FLC*, *MAF4*, *MAF5*, and *FT*

Because HDA9 localizes to the nuclei and many Rpd3/HDA1 class I HDACs in yeast, fly, and humans are present within various transcriptional repressor complexes (reviewed in Hayakawa & Nakayama, 2011), we questioned whether the *hda9-1* mutation affects the expression of key flowering genes at their mRNA level: *CO*, a key floral promoter in the photoperiod pathway; *FLC*, a central floral repressor in the autonomous and vernalization pathways, and its five paralogs (*MAF1* through *MAF5*); and the floral integrators *FT* and *SOC1*. Under both LD and SD conditions, *FLC* mRNA levels were slightly reduced in *hda9-1*, whereas *CO* mRNA levels in wt and *hda9-1* were comparable (Fig. 4a,b). Down-regulation of *MAF4* and *MAF5* mRNAs by *hda9-1* was also observed in the SD condition (Fig. 4b). Consistent with the early-flowering phenotype of *hda9-1*, *FT* and, to a much lesser extent, *SOC1* mRNA levels were higher in *hda9-1* than in the wt (Fig. 4a,b).

Because the genetic analysis positioned *FT* downstream of *HDA9*, we further examined the effect of *hda9-1* mutation on the spatial expression of *FT* using *FT::GUS* (Takada & Goto, 2003). Under LD conditions, GUS staining was detected mainly in the vascular tissues of the distal parts of both wt and *hda9-1* rosette leaves with similar staining intensity (Fig. 4c). Under SD conditions, GUS staining was detected in the primary veins and petioles of both wt and *hda9-1* leaves; however, a stronger intensity was observed in *hda9-1* than in the wt, which indicates that

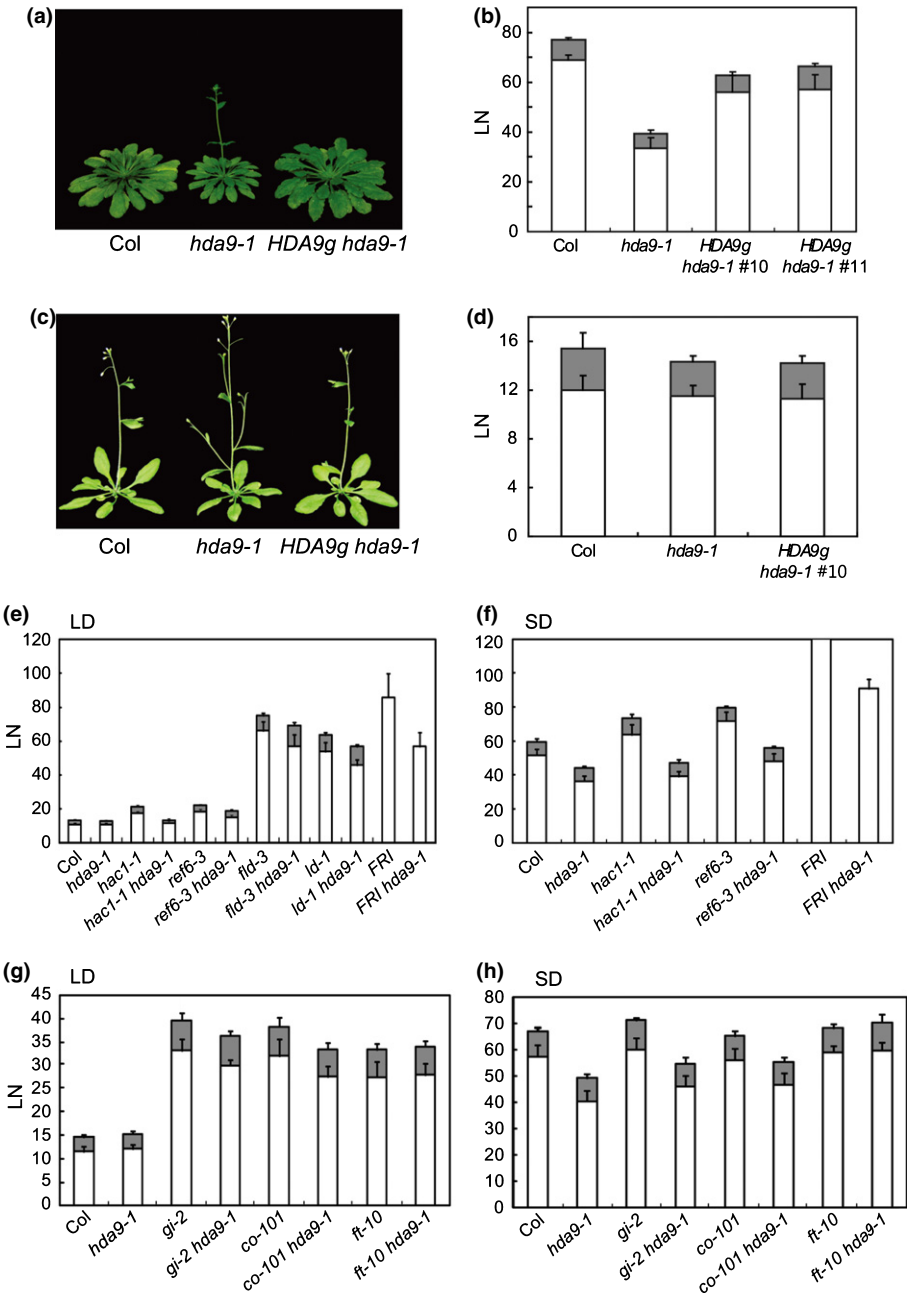

Fig. 3 The *Arabidopsis thaliana hda9-1* mutation causes early flowering. (a) Wild-type (wt) Col, *hda9-1*, and *HDA9g hda9-1* plants grown for 85 d under short-day (SD) conditions. (b) Flowering time of wt, *hda9-1*, and two independent *HDA9g hda9-1* transgenic lines under SD conditions. Flowering times were determined as the numbers of rosette (white bars) and cauline (gray bars) leaves formed at bolting (LN) and presented as means ± SD (b, d–h). (c) Wild-type, *hda9-1*, and *HDA9g hda9-1* plants grown for 25 d under long-day (LD) conditions. (d) Flowering time of wt, *hda9-1*, and an *HDA9g hda9-1* transgenic line under LD conditions as determined by LN. (e–h) Double mutant analyses of *hda9-1* with various late-flowering mutants of the autonomous (e, f) or photoperiod pathway (g, h). Flowering time was measured either under LD (e, g) or SD conditions (f, h) by scoring LN. The *FRI* plants grown under SDconditions (f) did not flower at the time of measurement and produced > 130 rosette leaves.

HDA9 affects the expression level but not the expression domain of *FT*. Collectively, these results show that *HDA9* is required for the full expression of *FLC*, *MAF4* and *MAF5*, and for the negative regulation of *FT*.

HDA9 controls flowering mostly independently of *FLC*, *MAF4*, and *MAF5*

FLOWERING LOCUS C directly binds to the *FT* and *SOC1* promoters and represses the transcription of *FT* and *SOC1* (Helliwell *et al.*, 2006). It is therefore possible that the up-regulation of *FT* and *SOC1* in *hda9-1* is the result of the reduced *FLC* expression. To test this possibility, we compared the flowering times of *hda9-1*, *flc-3* (an *FLC* null mutant; Michaels & Amasino, 2001), and the *flc-3 hda9-1* double mutants under SD conditions. The flowering time of *hda9-1* was similar to that of *flc-3* (Fig. 4d), although a substantial amount of *FLC* transcript was present in *hda9-1* (Fig. 4b). Moreover, compared with both single mutants, the *flc-3 hda9-1* double mutant flowered slightly earlier and had a higher abundance of *FT* transcript (Fig. 4d,e). *SOC1* expression in *flc-3 hda9-1* compared with either of the single mutants was not increased as substantially as *FT* (Fig. 4e). These results indicate that the reduced *FLC* expression alone is not sufficient to cause the early flowering of *hda9-1*.

Similar to *FLC*, *MAF4* and *MAF5* have also been implicated in floral repression (Ratcliffe *et al.*, 2003; Gu *et al.*, 2009). Thus,

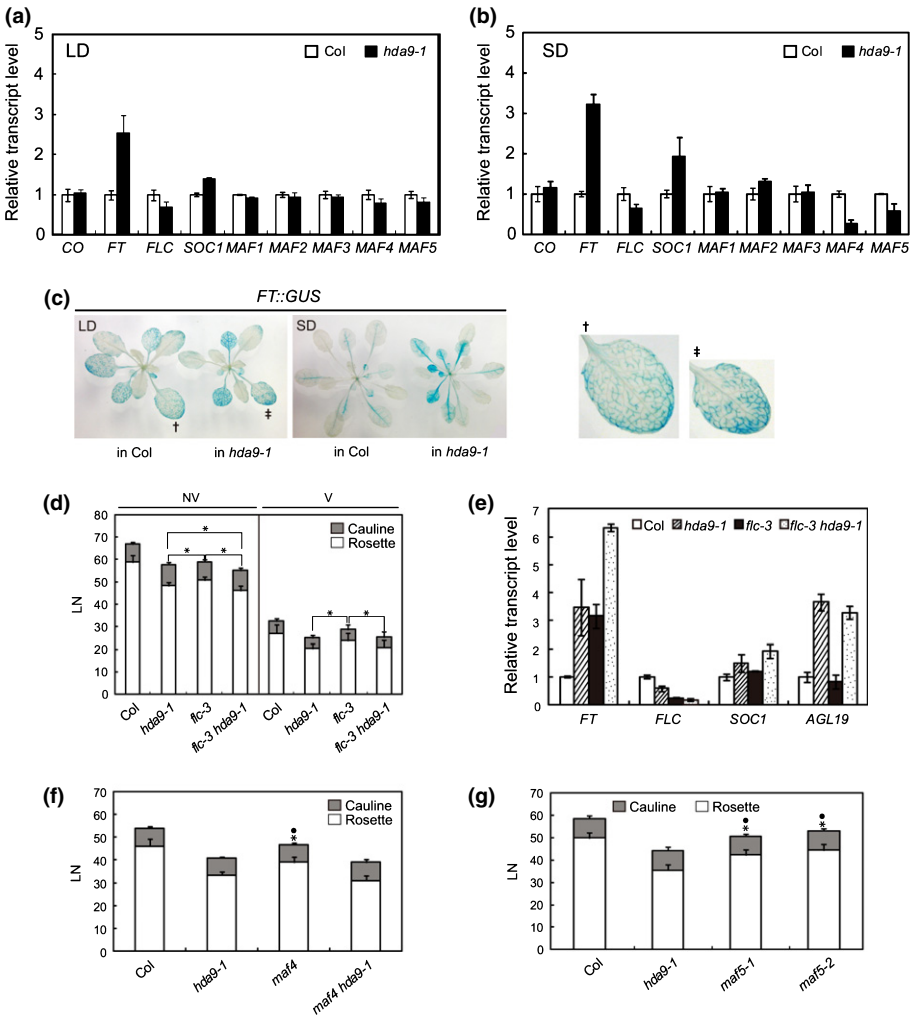

Fig. 4 The *Arabidopsis thaliana hda9-1* mutation affects *FT* expression. (a, b) Quantitative real-time reverse transcription polymerase chain reaction (RT-qPCR) analyses of the transcript abundances of various flowering genes in wild-type (wt) and *hda9-1* seedlings grown for 2 wk under long-day (LD) conditions (a) or 4 wk under short-day (SD) conditions (b). Wild-type levels were set to 1 after normalization by *UBQ10*. Values are the means ± SE of three biological replicates. (c) Histochemical β-glucuronidase (GUS) staining of wt and *hda9-1* plants harboring *FT::GUS*. Plants were grown for 21 d under LD or 45 d under SD conditions before staining. All the plants were homozygous for *FT::GUS*. Right panel, 300% digital magnification of the marked leaves on the left to show vascular expression of FT::GUS. (d) Flowering time of *hda9-1*, *flc-3* and *flc-3 hda9-1* without (NV) or with (V) vernalization as determined by bolting (LN). Vernalization was performed as described in the Materials and Methods section, and the plants were subsequently grown under SD conditions until bolting. Asterisks indicate statistically significant differences between the two comparisons marked by brackets ($P \leq 0.01$). (e) Additive effect of *flc-3* and *hda9-1* on *FT* expression. Plants were grown for 21 d under SD conditions before being harvested for RNA extraction. Transcript abundances of *FT*, *FLC*, *SOC1* and *AGL19* were determined by RT-qPCR, and wt levels were set to 1 after normalization by *UBQ10*. Values are the means ± SE of three biological replicates. (f) Flowering time of *hda9-1*, *maf4* and *maf4 hda9-1* under SD conditions as determined by LN. Closed circles or asterisks indicate statistically significant differences from Col or *hda9-1*, respectively ($P < 0.001$; f, g). (g) Flowering time of *hda9-1* and *maf5* mutants under SD conditions as determined by LN. Values are the means ± SD (d, f, g).

to examine whether the decreased expression of *MAF4* and *MAF5* contributes to the accelerated flowering of *hda9-1*, T-DNA insertion mutants of *MAF4* and *MAF5* (Fig. S5) were isolated from the SALK collection, and their flowering time was analyzed. Both *maf4* and *maf5* flowered slightly earlier than the wt but significantly later than *hda9-1* under SD conditions (Fig. 4f,g). In addition, the *maf4 hda9-1* double mutants flowered slightly earlier than the *maf4* or the *hda9-1* single mutants (Fig. 4f). Moreover, *flc-3 hda9-1* flowered earlier than *flc-3* even after vernalization (Fig. 4d), which should have decreased the expression of *MAF4* (Ratcliffe *et al.*, 2003). Thus, although the decreased expression of *MAF4* and *MAF5* might contribute to the early flowering of *hda9-1*, it does not seem to fully account for the flowering behavior observed in *hda9-1*. In sum, these results suggest that HDA9 controls flowering time mostly independently of *FLC*, *MAF4* and *MAF5*.

The expression of *AGL19*, a floral activator, is increased in *hda9-1*

A number of MADS- and AP2-domain transcription factors that affect flowering in an *FLC*-independent manner have been

identified (Yu *et al.*, 2002; Aukerman & Sakai, 2003; Michales *et al.*, 2003; Schmid *et al.*, 2003; Schönrock *et al.*, 2006; Adamczyk *et al.*, 2007; Jung *et al.*, 2007; Castillejo & Pelaz, 2008; Yoo *et al.*, 2011). In addition, it was recently shown that SPL transcription factors promote flowering independently of *FLC* (Wang *et al.*, 2009a). To study whether HDA9 affects flowering by regulating these factors, we compared their expression levels in wt and *hda9-1*. All the genes examined, with the exception of *AGL19*, were expressed at similar levels in the wt and *hda9-1* (Figs 5a, S6). Interestingly, under both LD and SD photoperiods, the transcript abundance of *AGL19* was substantially higher in *hda9-1* than in the wt (Figs 5a, S6). The up-regulation of *AGL19* is not thought to be related to the reduced *FLC* expression in *hda9-1*, because the expression of *AGL19* was not affected by *flc-3* (Fig. 4e). We found that the transcript abundance of *AGL19*, similar to *FT*, was greatly elevated in 5-wk-old plants compared with 1-wk-old seedlings (Fig. 5b,c), consistent with previous reports on the age-dependent induction of *AGL19* (Schönrock *et al.*, 2006). Interestingly, the effect of the *hda9-1* mutation on *AGL19* expression was barely detectable in young seedlings, although it became obvious in 5-wk-old plants (Fig. 5b).

HDA9 directly represses *AGL19* transcription through histone deacetylation

The increased expression of *AGL19*, *FT*, and *SOC1* by the loss of *HDA9* led us to test whether HDA9 directly represses the transcription of these genes by deacetylating histones within *AGL19* or *FT* chromatin. ChIP studies using anti-acetylated histone H3 (H3Ac) antibody showed that H3Ac levels at the *AGL19* locus were comparable between the wt and *hda9-1* in 1-wk-old seedlings (Fig. 5d,e). However, H3Ac levels around the transcription start site of *AGL19* (regions D, E, I, II and III) were clearly increased in 5-wk-old *hda9-1* but not in wt plants compared with the levels observed in 1-wk-old seedlings (Fig. 5d,e). In contrast to *AGL19*, there was no clear difference in H3Ac levels at *FT* and *SOC1* loci between wt and *hda9-1* at both the seedling and mature stages (Figs 5d,f, S7a,b). Given the fact that the transcript abundances of both *AGL19* and *FT* were developmentally increased and up-regulated by the loss of *HDA9* (Fig. 5b,c), these results suggest that the hyperacetylation of histones within *AGL19* chromatin in *hda9-1* is not merely a consequence of the increased *AGL19* transcription. Instead, it might be the result of decreased HDAC activity caused by the loss of *HDA9*.

To study whether the increased *AGL19* mRNA levels and the hyperacetylation of histones within *AGL19* chromatin in *hda9-1* are related to increased transcriptional activity, we compared RNA polymerase II (PolII) occupancies at *AGL19* in the wt and *hda9-1* through ChIP assays using an anti-PolII antibody. The PolII occupancy at *AGL19* was higher in *hda9-1* than in the wt; in addition, the occupancy pattern was closely correlated with that of H3Ac (Fig. 5g). The PolII occupancy in the regions around the transcription start site (I, II and III), but not in the elongation or termination regions (IV and V), was clearly higher in *hda9-1* than in the wt. These results suggest that the histone hyperacetylation in the promoter and 5′ transcribed regions of *AGL19* might increase the accessibility of these regions to PolII, which in turn accelerates transcription.

Finally, in order to address whether HDA9 plays a direct role in the transcriptional regulation of *AGL19*, we performed ChIP assays using *HDA9:HA hda9-1* plants (Fig. S4). HDA9:HA protein was clearly enriched within *AGL19* (Fig. 5h) but not within *SOC1* chromatin (Fig. S7c), consistent with the effect of the *hda9-1* mutation on H3Ac levels at these loci (Figs 5e, S7b). HDA9:HA enrichment was most obvious in regions upstream of the transcription start site of *AGL19*. Thus, HDA9 has a direct role in controlling and maintaining the transcription activity of *AGL19* at a proper level by resetting the local chromatin environment through dynamic histone deacetylation.

HDA9 controls *FT* expression and flowering through *AGL19*

The correlation between the transcript and H3Ac levels of *AGL19* but not of *FT* and *SOC1* (Figs 4b, 5b–f, S7b) led us to question whether the up-regulation of *FT*/*SOC1* and the accelerated floral transition in *hda9-1* are caused by the increased *AGL19* expression. We thus measured the mRNA levels of *FT* and *SOC1* in wt, *hda9-1*, *agl19-1*, and transgenic plants overexpressing *AGL19* (*AGL19OE*; Schönrock *et al.*, 2006). *AGL19OE* was previously shown to have early-flowering phenotypes under both LD and SD conditions (Schönrock *et al.*, 2006). The *FT* mRNA level was greatly increased when *AGL19* was

Fig. 5 *Arabidopsis thaliana* HDA9 directly controls *AGL19* transcription through histone deacetylation. (a) Quantitative real-time reverse transcription polymerase chain reaction (RT-qPCR) analyses of the transcript abundances of several *AGL* genes, which have floral regulatory roles, in wild-type (wt) and *hda9-1* seedlings grown for 2 wk under LD (left) or 4 wk under SD conditions (right). Wild-type levels were set to 1 after normalization by *UBQ10*, and values are the means ± SE of three biological replicates (a–c, h). (b, c) Transcript abundances of *AGL19* (b) or *FT* (c) in 1-wk-old (SD1w) or 5-wk-old (SD5w) wt and *hda9-1* plants grown under SD conditions as determined by RT-qPCR. (d) Schematics of the genomic structures of *AGL19* and *FT*. Gray boxes, 5′ and 3′ untranslated regions; white boxes, exons; solid lines, promoters, introns, or intergenic regions; + 1, transcription start sites. Regions amplified by primers used for chromatin immunoprecipitation (ChIP) (e–g) are shown for each gene. (e, f) ChIP-qPCR analyses of *AGL19* (e) and *FT* (f) chromatin using an anti-H3Ac antibody. Plants as grown in (b) and (c) were used for ChIP. Shown are the means ± SE of three biological replicates. SD1w wt levels were set to 1 after normalization by input and the internal control *UBQ10*. (g) ChIP-qPCR analyses of *AGL19* chromatin with an anti-PolII antibody. Plants grown for 5 wk under SD conditions were used for ChIP. Shown are the means ± SE of three biological replicates. Wild-type levels were set to 1 after normalization by input. *Actin 2/7* (*ACT2/7*) and *UBQ10* were used as internal controls. (h) ChIP-qPCR analyses of HDA9:HA enrichment at the *AGL19* locus using an anti-HA antibody. *HDA9:HA hda9-1* and *hda9-1* plants grown for 5 wk under SD conditions were used for ChIP. The amount of immunoprecipitated chromatin was normalized to the corresponding input and compared with untagged plants. Shown are the means ± SE of three biological replicates.

overexpressed and was not largely affected by *agl19-1* (Schönrock *et al.*, 2006; Fig. 6a). However, the mRNA levels of *FLC* and *SOC1* were barely affected by differential *AGL19* expression (Fig. 6a), indicating that the up-regulation of *FT* in *AGL19OE* is independent of *FLC*. These results suggest that the repressive effect of *HDA9* on *FT* might be, at least in part, through the inhibition of *AGL19* transcription. Therefore, we analyzed the effect of the *agl19* mutation on the early flowering of *hda9-1* by

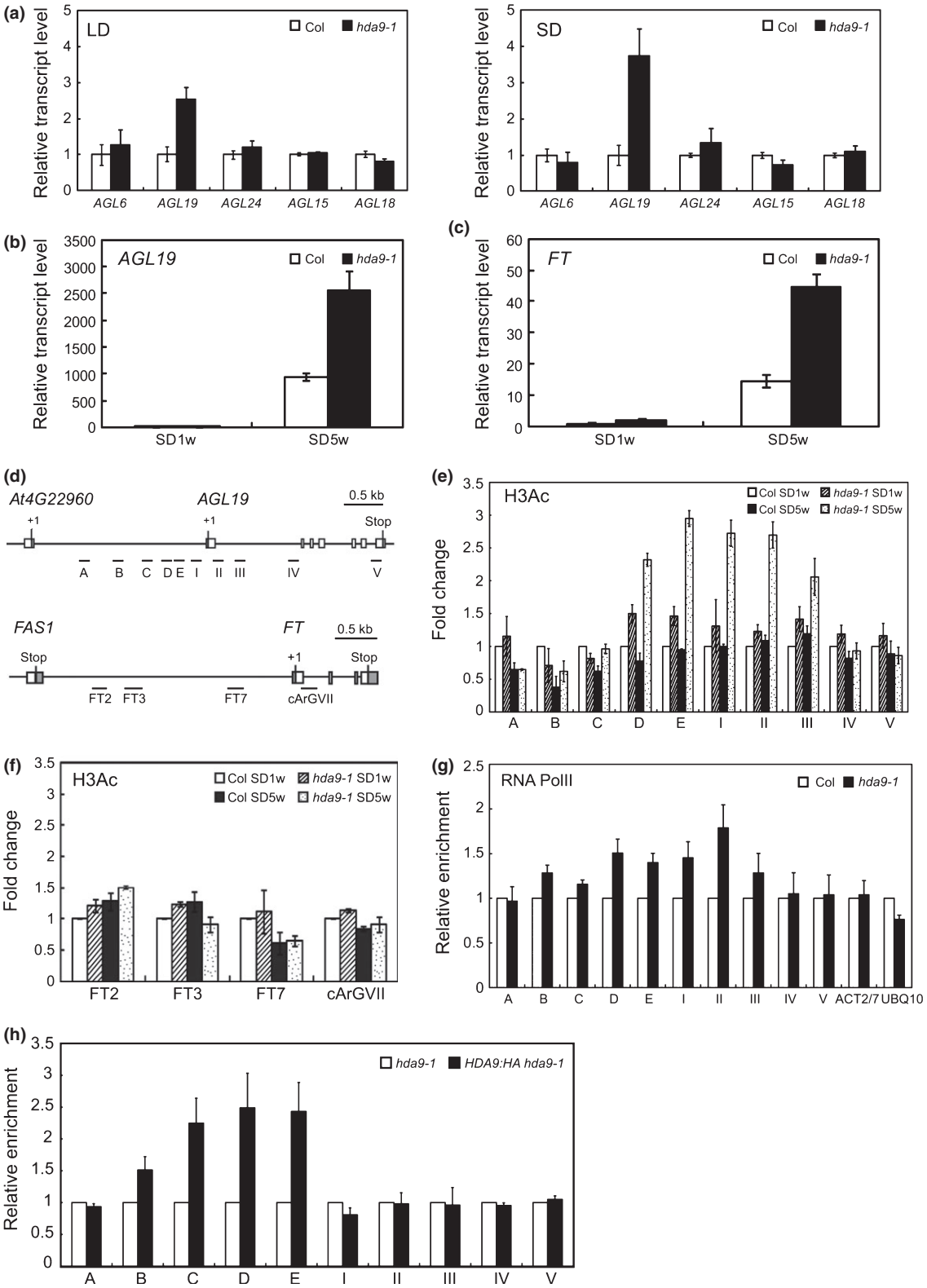

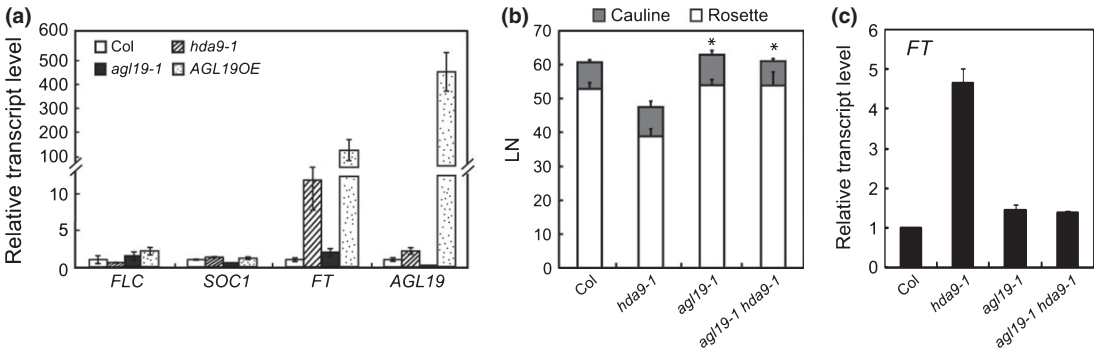

Fig. 6 *Arabidopsis thaliana* HDA9 affects *FT* expression and flowering through *AGL19*. (a) Quantitative real-time reverse transcription polymerase chain reaction (RT-qPCR) analyses of the transcript abundances of *FLC*, *SOC1*, *FT* and *AGL19* in *hda9-1*, *agl19-1*, and *AGL19OE* plants. Plants grown for 3 wk under short-day (SD) conditions were used for RNA extraction. (b) Flowering time of *hda9-1*, *agl19-1*, and *agl19-1 hda9-1* mutant plants under SD conditions as determined by bolting (LN). Asterisks denote statistically significant differences from *hda9-1* ($P < 0.001$). Values are means ± SD. (c) *FT* transcript abundances as determined by RT-qPCR in *hda9-1*, *agl19* and *agl19-1 hda9-1* mutant plants grown for 13 wk under SD conditions. The wt level was set to 1 after normalization by *UBQ10*, and values are the means ± SE of three technical replicates (a, c).

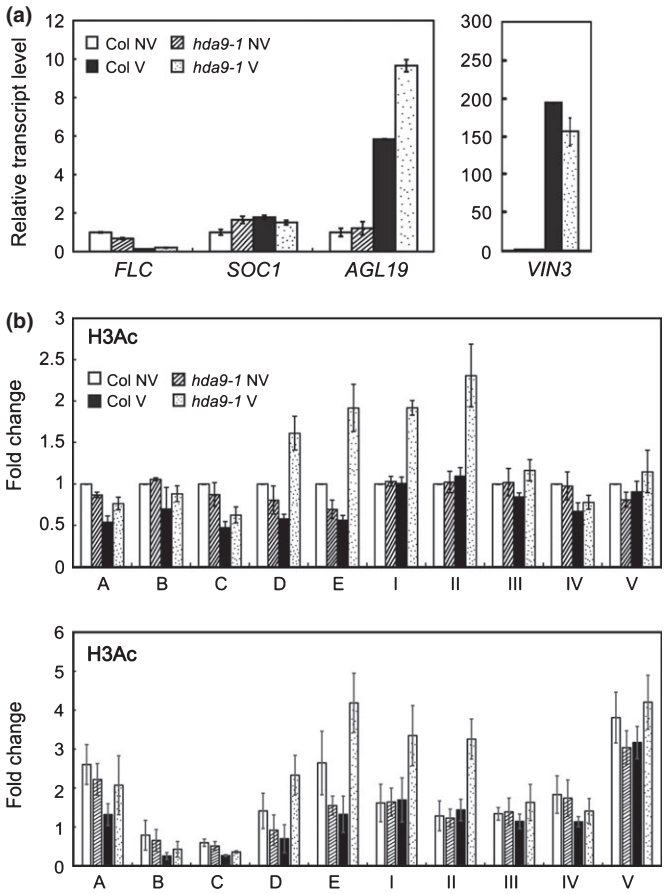

Fig. 7 Hyperacetylation of histones within *AGL19* chromatin by the *Arabidopsis thaliana hda9-1* mutation in vernalized seedlings. (a) Quantitative real-time reverse transcription polymerase chain reaction (RT-qPCR) analyses of the transcript abundances of *FLC*, *SOC1*, *AGL19* and *VIN3* in wild-type (wt) and *hda9-1* seedlings vernalized for 30 d (V) or not vernalized (NV). NV wt levels were set to 1 after normalization by *UBQ10*. Values are the means ± SE of three biological replicates. (b) Chromatin immunoprecipitation (ChIP)-qPCR analyses of *AGL19* chromatin using an anti-H3Ac antibody. Plants were grown as described in (a). NV wt levels were set to 1 (upper) or not (lower) after normalization by input and the internal control *UBQ10*. Shown are the means ± SE of three biological replicates.

measuring the flowering time of the *agl19-1 hda9-1* double mutants. *agl19-1 hda9-1* flowered at a similar time as the wt but significantly later than the *hda9-1* single mutants (Fig. 6b), clearly demonstrating that *AGL19* is required for the early flowering of *hda9-1*. Furthermore, the increased expression of *FT* in *hda9-1* was strongly suppressed by the *agl19-1* mutation (Fig. 6c). By contrast, the up-regulated *SOC1* expression in *hda9-1* was not suppressed by the *agl19-1* mutation (Fig. S7d). Thus, we concluded that HDA9 prevents precocious flowering under SD conditions mostly by inhibiting *AGL19* up-regulation, which would otherwise, in turn, activate *FT*.

Loss of *HDA9* increases the levels of *AGL19* mRNA and H3Ac at *AGL19* in vernalized seedlings

Previous work showed that *AGL19* mRNA expression is induced by vernalization (Schönrock *et al.*, 2006). Therefore, we examined the effect of the *hda9-1* mutation on the vernalization-induced *AGL19* expression (Fig. 7a). In nonvernalized seedlings, the *AGL19* mRNA level was low and similar in both wt and *hda9-1* plants. However, after 4 wk of vernalization, it was increased in the wt and, notably, to a greater extent, in *hda9-1*. The hyperinduction of the vernalization-mediated *AGL19* expression by the *hda9-1* mutation might account for the accelerated floral transitions of *hda9-1* and *flc-3 hda9-1* compared with *flc-3* (Fig. 4d). We then studied H3Ac levels at *AGL19* in wt and *hda9-1* seedlings before and after vernalization (Fig. 7b). There was no detectable difference in H3Ac levels at *AGL19* between nonvernalized wt and *hda9-1* seedlings. However, an evident increase in H3Ac levels at *AGL19*, especially in regions around the transcription start site, was detected in *hda9-1* but not in wt after vernalization. Thus, the results in Fig. 7 indicate that HDA9 also prevents the hyperactivation of *AGL19* transcription during vernalization through a dynamic histone deacetylation.

AGL19 is differentially expressed in different photoperiods

We then questioned whether the regulation of *AGL19* by HDA9 is relevant to the photoperiod-dependent early-flowering

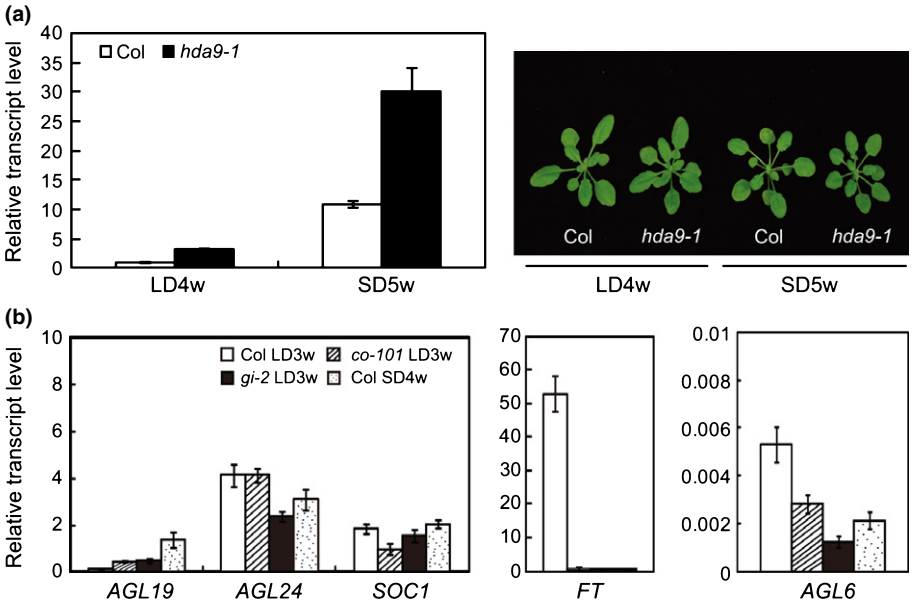

Fig. 8 Photoperiod-dependent expression of *Arabidopsis thaliana AGL19*. (a) Quantitative real-time reverse transcription polymerase chain reaction (RT-qPCR) analyses of *AGL19* transcript abundances in wild-type (wt) and *hda9-1* plants grown for 4 wk under long-day (LD) conditions (LD4w) or for 5 wk under short-day (SD) conditions (SD5w). The picture on the right shows representative wt and *hda9-1* plants. The LD4w wt level was set to 1 after normalization by *UBQ10*. Values are means ± SE of three biological replicates. (b) RT-qPCR analyses of the transcript abundances of *AGL19*, *AGL24*, *SOC1*, *FT* and *AGL6* in wt, *co-101* and *gi-2* plants grown for 3 wk under LD conditions (LD3w) or 4 wk under SD conditions (SD4w). Transcript abundances of each gene were normalized by *UBQ10*, and values are the means ± SE of three biological replicates.

phenotype of *hda9-1*. Interestingly, *AGL19* mRNA levels were *c.* 10-fold higher in 5-wk-old SD-grown plants than in 4-wk-old LD-grown plants regardless of the *HDA9* genotype (Fig. 8a). This difference in *AGL19* expression is unlikely to be the result of the age difference between the LD- and SD-grown plants, because the 4-wk-old LD-grown plants were rather developmentally more progressed than the 5-wk-old SD-grown plants (Fig. 8a). Thus, *AGL19* might be expressed only in SD-grown *hda9-1* plants to the level required for the activation of *FT* and precocious flowering, and this might be the cause of the SD-specific early flowering of *hda9-1*.

Notably, *AGL19* expression was less affected by the loss of *CO* or *GI* under LD conditions than by SD conditions (Fig. 8b). The *AGL19* mRNA level in 3-wk-old LD-grown *gi-2* or *co-101* mutants was moderately higher than that in 3-wk-old LD-grown wt plants, but substantially lower than that in 4-wk-old SD-grown wt plants. Thus, unlike *FT* (Fig. 8b), the photoperiodic regulation of *AGL19* is largely independent of the GI–CO pathway. This result is in agreement with our observations that the suppressive effect of the *hda9-1* mutation on the late flowering of *co-101* or *gi-2* in LD (Fig. 3g) was weaker than its effect in SD (Fig. 3h). Taken together, these results suggest that the repressive role of HDA9 in *AGL19* expression together with the photoperiod-dependent expression of *AGL19* might underlie the SD-specific early flowering of the *hda9-1* mutants.

Discussion

Arabidopsis has a higher number of HDACs than other multicellular eukaryotes; however, to date, the biological roles of individual Arabidopsis HDACs, with the exception of HDA6 and HDA19, are mostly unknown. In this study, we show that HDA9, an Arabidopsis RPD3/HDA1 family class I HDAC, plays distinct roles in plant development. The loss of *HDA9* causes several morphological alterations in a limited number of organs (Fig. 1), none of which are observed in the *hda6* or *hda19* mutants. These observations suggest that the *in planta* function of HDA9 might be localized and not global and that this function does not overlap with the functions of HDA6 or HDA19. It would be interesting to know how HDA9 and its phylogenetically close members, HDA6 and HDA19, perform distinct biological roles despite their conserved HDAC activity. The specificity of these HDACs might lie in their participation in different multiprotein complexes. Studies on animal and yeast HDACs have shown that most class I HDACs perform their functions within a variety of multiprotein complexes, each of which has different target range (Cunliffe, 2008; reviewed in Yang & Seto, 2008). Although, to our knowledge, no HDAC complex has yet been biochemically purified from Arabidopsis, Arabidopsis HDACs are also likely to interact with different proteins or complexes, which might lead to different biological effects. Therefore, biochemical purification of HDA9-containing complexes will provide a better understanding of the action mechanisms of HDA9 and insights into its target specificity.

Our study using *hda9-1* revealed that HDA9 is involved in the control of flowering time, especially under noninductive SD conditions. Floral repression in SD is as important as floral promotion in LD for the reproductive success of a facultative LD plant, such as Arabidopsis. Precocious flowering of a number of loss-of-

function mutants, such as *emf2* (Kim *et al.*, 2010) and *flm* (Gu *et al.*, 2013), under SD conditions suggests that the repressive mechanisms to attenuate floral competence as well as the lack of floral promoter activity of the CO–FT pathway contribute to the repression of flowering in Arabidopsis under SD conditions. Our data indicate that HDA9 contributes to this floral repression mainly by negatively regulating the expression *AGL19*, an *FT* activator (Figs 5, 6). *AGL19* appears to be responsible for the SD-specific early flowering of *hda9-1* as well. *AGL19* expression is higher in SD than in LD (Fig. 8a), and its low level of expression in *hda9-1* under LD conditions may not be sufficient to effectively activate *FT* (Fig. 8b). Thus, in addition to strong CO activity, the low level of *AGL19* expression might be responsible for the normal flowering behavior of the *hda9-1* mutants under LD conditions. The role of *AGL19* in promoting floral transition in the wt is likely redundant or its expression level in wt is not sufficient for effective *FT* activation, because its loss-of-function mutants displayed a normal flowering behavior without reduced *FT* expression in SD (Fig. 6b,c). In either case, ensuring the proper expression of *AGL19* during the developmental time course is crucial for the prevention of precocious flowering under noninductive SD conditions. In sum, the control of *AGL19* expression by HDA9 adds a new layer to the mechanisms that prevent precocious flowering in SD.

Conventionally, the role of HDACs has been thought to be associated with inactive genes. However, the *hda9-1* mutation-induced increase of H3Ac levels at *AGL19* was clearly observed only at times when *AGL19* was actively expressed, such as in the adult stages or after vernalization (Figs 5e, 7b). Thus, the role of HDA9 at *AGL19* is distinct from the conventional corepressor role of HDACs. Interestingly, a recent genome-wide mapping of HDACs in human CD4+ cells showed that HDACs associate more with transcriptionally active genes than with inactive genes (Wang *et al.*, 2009b), which suggests a novel role for HDACs during transcription. Increased H3Ac levels at *AGL19* in *hda9-1* but not in the wt during development under SD conditions (Fig. 5e) implies that acetyl groups may be dynamically added to the histone tails and reversibly removed by HDA9 during the transcription of *AGL19*. This HDA9 function might be important in the prevention of hyperactive transcription by resetting the chromatin state. This postulate is supported by the *hda9-1* mutation-induced increase in PolII occupancy, which is correlated with increased H3Ac levels in regions surrounding the *AGL19* transcription start site (Fig. 5g). Histone hyperacetylation in these regions might cause hyperactive transcription at premature developmental stages. It will be of interest in the future to determine whether HDA9 has a similar role in the control of other genes during their transcription.

Acknowledgements

This work was supported by a grant from the National Research Foundation (NRF-2013R1A2A1A01010750) and by the Next-Generation BioGreen21 Program (PJ008206 and PJ009580) of the Rural Development Administration.

References

Adamczyk BJ, Lehti-Shiu MD, Fernandez DE. 2007. The MADS domain factors AGL15 and AGL18 act redundantly as repressors of the floral transition in Arabidopsis. *Plant Journal* **50**: 1007–1019.

Amasino R. 2010. Seasonal and developmental timing of flowering. *Plant Journal* **61**: 1001–1013.

Aufsatz W, Mette MF, van der Winden J, Matzke M, Matzke AJM. 2002. HDA6, a putative histone deacetylase needed to enhance DNA methylation induced by double-standard RNA. *EMBO Journal* **21**: 6832–6841.

Aukerman MJ, Sakai H. 2003. Regulation of flowering time and floral organ identity by a MicroRNA and its APETALA2-like target genes. *Plant Cell* **15**: 2730–2741.

Benhamed M, Bertrand C, Servet C, Zhou DX. 2006. Arabidopsis GCN5, HD1, and TAF1/HAF2 interact to regulate histone acetylation required for light-responsive gene expression. *Plant Cell* **18**: 2893–2903.

Blázquez MA, Weigel D. 2000. Integration of floral inductive signals in Arabidopsis. *Nature* **404**: 889–892.

Castillejo C, Pelaz S. 2008. The balance between CONSTANS and TEMPRANILLO activities determines *FT* expression to trigger flowering. *Current Biology* **18**: 1338–1343.

Choi SM, Song HR, Han SK, Han M, Kim CY, Park J, Lee YH, Jeon JS, Noh YS, Noh B. 2012. HDA19 is required for the repression of salicylic acid biosynthesis and salicylic acid-mediated defense responses in Arabidopsis. *Plant Journal* **71**: 135–146.

Clough SJ, Bent AF. 1998. Floral dip: a Simplified method for Agrobacterium-mediated transformation of *Arabidopsis thaliana*. *Plant Journal* **16**: 735–743.

Cunliffe VT. 2008. Eloquent silence: developmental functions of Class I histone deacetylases. *Current Opinion in Genetics & Development* **18**: 404–410.

Earley K, Lawrence RJ, Pontes O, Reuther R, Enciso A, Silva M, Neves N, Gross M, Viegas W, Pikaard CS. 2006. Erasure of histone acetylation by Arabidopsis HDA6 mediates large-scale gene silencing in nucleolar dominance. *Genes & Development* **20**: 1283–1293.

Earley KW, Pontvianne F, Wierzbicki AT, Blevins T, Tucker S, Costa-Nunes P, Pontes O, Pikaard CS. 2010. Mechanisms of HDA6-mediated rRNA gene silencing: suppression of intergenic Pol II transcription and differential effects on maintenance versus siRNA-directed cytosine methylation. *Genes & Development* **24**: 1119–1132.

Fong PM, Tian L, Chen J. 2006. *Arabidopsis thaliana* histone deaetylase 1 (AtHD1) is localized in euchromatic regions and demonstrates histone deacetylase activity *in vitro*. *Cell Research* **16**: 479–488.

Grozinger CM, Schreiber SL. 2000. Regulation of histone deacetylase 4 and 5 and transcriptional activity by 14-3-3-dependent cellular localization. *Proceedings of the National Academy of Sciences, USA* **97**: 7835–7840.

Gu X, Jiang D, Wang Y, Bachmair A, He Y. 2009. Repression of the floral transition via histone H2B monoubiquitination. *Plant Journal* **57**: 522–533.

Gu X, Le C, Wang Y, Li Z, Jiang D, Wang Y, He Y. 2013. *Arabidopsis* FLC clade members form flowering-repressor complexes coordinating responses to endogenous and environmental cues. *Nature Communications* **4**: 1947.

Han SK, Song JD, Noh YS, Noh B. 2007. Role of plant CBP/p300-like genes in the regulation of flowering time. *Plant Journal* **49**: 103–114.

Hayakawa T, Nakayama J. 2011. Physiological roles of Class I HDAC complex and histone demethylases. *Journal of Biomedicine and Biotechnology* **2011**: 1–10.

He Y, Michaels SD, Amasino RM. 2003. Regulation of flowering time by histone acetylation in Arabidopsis. *Science* **302**: 1751–1754.

Helliwell CA, Wood CC, Robertson M, Peacock WJ, Dennis ES. 2006. The Arabidopsis FLC protein interacts directly *in vivo* with *SOC1* and *FT* chromatin and is a part of a high-molecular-weight protein complex. *Plant Journal* **46**: 183–192.

Hollender C, Liu Z. 2008. Histone deacetylase genes in Arabidopsis development. *Journal of Integrative Plant Biology* **50**: 875–885.

Jung JH, Seo YH, Seo PJ, Reyes JL, Yun J, Chua NH, Park CM. 2007. The GIGANTEA-regulated microRNA172 mediates photoperiodic flowering independent of CONSTANS in Arabidopsis. *Plant Cell* **19**: 2736–2748.

Kaufmann K, Muiño JM, Østerås M, Farinelli L, Krajewski P, Angenent GC. 2010. Chromatin immunoprecipitation (ChIP) of plant transcription factors followed by sequencing (ChIP-SEQ) or hybridization to whole genome arrays (ChIP-CHIP). *Nature Protocol* **5**: 457–472.

Kim W, Latrasse D, Servet C, Zhou DX. 2013. Arabidopsis histone deacetylase HDA9 regulates flowering time through repression of AGL19. *Biochemical and Biophysical Research Communications* **432**: 394–398.

Kim DH, Sung S. 2010. The Plant Homeo Domain finger protein, VIN3-LIKE 2, is necessary for photoperiod-mediated epigenetic regulation of the floral repressor, MAF5. *Proceedings of the National Academy of Sciences, USA* **107**: 17029–17034.

Kim KC, Lai Z, Fan B, Chen Z. 2008. *Arabidopsis* WRKY38 and WRKY62 transcription factors interact with histone deacetylase 19 in basal defense. *Plant Cell* **20**: 2357–2371.

Kim SY, Zhu T, Sung ZR. 2010. Epigenetic regulation of gene programs by EMF1 and EMF2 in Arabidopsis. *Plant Physiology* **152**: 516–528.

Kinkema M, Fan W, Dong X. 2000. Nuclear localization of NPR1 is required for activation of *PR* gene expression. *Plant Cell* **12**: 2339–2350.

Koornneef M, Alonso-Blanco C, Peeters AJM, Soppe W. 1998. Genetic control of flowering time in Arabidopsis. *Annual Review of Plant Physiology and Plant Molecular Biology* **49**: 345–370.

Koornneef M, Vrles HB, Hanhart C, Soppe W, Peeters T. 1994. The phenotype of some late-flowering mutants is enhanced by a locus on chromosome 5 that is not effective in the Landsberg erecta wild-type. *Plant Journal* **6**: 911–919.

Kurdistani SK, Robyr D, Tavazoie S, Grunstein M. 2002. Genome-wide binding map of the histone deacetylase Rpd3 in yeast. *Nature Genetics* **31**: 248–254.

Lee I, Michaels SD, Amasino RM. 1994. The late-flowering phenotype of *FRIGIDA* and mutations in *LUMINIDEPENDENS* is suppressed in the Landsberg *erecta* strain of Arabidopsis. *Plant Journal* **6**: 903–909.

Liu X, Yu CW, Duan J, Luo M, Wang K, Tian G, Cui Y, Wu K. 2012. HDA6 directly interacts with DNA methyltransferase MET1 and maintains transposable element silencing in Arabidopsis. *Plant Physiology* **158**: 119–129.

Livak KJ, Schmittgen TD. 2001. Analysis of relative gene expression data using real-time quantitative PCR and the $2^{-\Delta\Delta CT}$ method. *Methods* **25**: 402–408.

Long JA, Ohno C, Simth ZR, Meyerowitz EM. 2006. TOPLESS regulates apical embryonic fate in *Arabidopsis*. *Science* **312**: 1520–1523.

Michaels SD, Amasino RM. 2001. Loss of *FLOWERING LOCUS C* activity eliminates the late flowering of *FRIGIDIA* and autonomous pathway mutants but not responsiveness to vernalization. *Plant Cell* **13**: 935–941.

Michales SD, Ditta G, Gustafson-Brown C, Pelaz S, Yanofsky M, Amasino R. 2003. *AGL24* acts as a promoter of flowering in *Arabidopsis* and is positively regulates by vernalization. *Plant Journal* **33**: 867–874.

Moon J, Suh SS, Lee H, Choi KR, Hong CB, Paek NC, Kim SG, Lee I. 2003. The *SOC1* MADS-box gene integrates vernalization and gibberellin signals for flowering in Arabidopsis. *Plant Journal* **35**: 613–623.

Noh B, Lee SH, Kim HJ, Yi G, Shin EA, Lee M, Jung KJ, Doyle MR, Amasino RM, Noh YS. 2004. Divergent roles of a pair of homologous jumonji/zinc-finger-class transcription factor proteins in the regulation of Arabidopsis flowering time. *Plant Cell* **16**: 2601–2613.

Noh B, Murphy AS, Spalding EP. 2001. *Multidrug resistance*-like genes of Arabidopsis required for auxin transport and auxin-mediated development. *Plant Cell* **13**: 2441–2454.

Pandey R, Muller A, Napoli CA, Selinger DA, Pikarrd CS, Richard EJ, Bender J, Mount DW, Jorgensen A. 2002. Analysis of histone acetyltransferase and histone deacetylase families of *Arabidopsis thaliana* suggests functional diversification of chromatin modification among multicellular eukaryotes. *Nucleic Acids Research* **30**: 5036–5055.

Park DH, Somers DE, Kim YS, Choy YH, Lim HK, Soh MS, Kim HJ, Kay SA, Nam HG. 1999. Control of circadian rhythms and photoperiodic flowering by the Arabidopsis *GIGANTEA* gene. *Science* **285**: 1579–1582.

Perales M, Màs P. 2007. A functional link between rhythmic changes in chromatin structure and the Arabidopsis biological clock. *Plant Cell* **19**: 2111–2123.

Probst AV, Fagard M, Proux F, Mourrain P, Boutet S, Earley K, Lawrence RJ, Pikkard CS, Murfett J, Furner I *et al.* 2004. Arabidopsis histone deacetylase *HDA6* is required for maintenance of transcriptional silencing and determines nuclear organization of rDNA repeats. *Plant Cell* **16**: 1021–1034.

Ratcliffe OJ, Kumimoto RW, Wong BJ, Riechmann JL. 2003. Analysis of the Arabidopsis *MADS AFFECTING FLOWERING* gene family: *MAF2* prevents vernnalization by short periods of cold. *Plant Cell* **15**: 1159–1169.

Schmid M, Uhlenhaut NH, Godard F, Demar M, Bressan R, Weigel D, Lohmann JU. 2003. Dissection of floral induction pathways using global expression analysis. *Development* **130**: 6001–6012.

Schönrock N, Bouveret R, Leroy O, Borghi L, Kohler C, Gruissem W, Hennig L. 2006. Plycomb-group proteins repress the floral activator *AGL19* in the *FLC*-independent vernalization pathway. *Genes & Development* **20**: 1667–1678.

Sung S, Schmitz RJ, Amasino RM. 2006. A PHD finger domain involved in both the verrnalization and photoperiod pathways in Arabidopsis. *Genes & Development* **20**: 3244–3248.

Takada S, Goto K. 2003. TERMINAL FLOWER 2, a HETEROCHROMATIN PROTEION1-Like protein of Arabidopsis, counteracts the activation of *FLOWERING LOCUS T* by CONSTANTS in the vascular tissues of leaves to regulate flowering time. *Plant Cell* **15**: 2856–2865.

Tanaka M, Kikuchi A, Kamada H. 2008. The Arabidopsis histone deacetylases HDA6 and HDA19 contribute to the repression of embryonic properties after germination. *Plant Physiology* **146**: 149–161.

Tian L, Chen ZL. 2001. Blocking histone deacetylation in Arabidopsis induces pleiotropic effects on plant gene regulation and development. *Proceedings of the National Academy of Sciences, USA* **98**: 200–205.

Tian L, Fong MP, Wang JJ, Wei NE, Jianf J, Doerge RW, Chen ZJ. 2005. Reversible histone acetylation and deacetylation mediate genome0wide, promoter-dependent and locus-specific changes in gene expression during plant development. *Genetics* **169**: 337–345.

Tian L, Wang J, Fong MP, Chen M, Cao H, Gelvin SB, Chen ZJ. 2003. Genetic control of developmental changes induced by disruption of Arabidopsis histone deacetylase 1 (AtHD1) expression. *Genetics* **165**: 399–409.

To TK, Kim JM, Matsui A, Kurihara Y, Morosawa T, Ishida J, Tanaka M, Endo T, Kakutani T, Toyoda T *et al.* 2011. Arabidopsis HDA6 regulates locus-directed heterochromatin silencing in cooperation with MET1. *PLoS Genetics* **7**: e1002055.

Torii KU, Mitsukawa N, Oosummi T, Matsuura Y, Yokoyamma R, Whittier RF, Komeda Y. 1996. The Arabidopsis *ERECTA* gene encodes a putative receptor protein kinase with extracellular kinase leucine-rich repeats. *Plant Cell* **8**: 735–746.

Turck F, Fornara F, Coupland G. 2008. Regulation and identity of florigen: FLOWERING LOCUS T moves center stage. *Annual Review of Plant Biology* **59**: 573–594.

Verdel A, Curtet S, Brocard MP, Rousseaux S, Lemercier C, Yoshida M, Khochbin S. 2000. Active maintenance of mHDA2/mHDA6 histone-deacetylase in the cytoplasm. *Current Biology* **10**: 747–749.

Wang Z, Zang C, Cui K, Schones DE, Barski A, Peng W, Zhao K. 2009b. Genome-wide mapping of HATs and HDACs reveals distinct functions in active and inactive genes. *Cell* **138**: 1019–1031.

Wang JW, Czech B, Weigel D. 2009a. miR156-regulated SPL transcription factors define an endogenous flowering pathway in *Arabidopsis thaliana*. *Cell* **138**: 738–749.

Wu K, Zhang L, Zhou C, Yu CW, Chaikam V. 2008. HDA6 is required for jasmonate response, senescence and flowering in Arabidopsis. *Journal of Experimental Botany* **59**: 225–234.

Xu CR, Liu C, Wang YL, Li LC, Chen WQ, Xu ZH, Bai SN. 2005. Histone acetylation affects expression of cellular patterning genes in the Arabidopsis root epidermis. *Proceedings of the National Academy of Sciences, USA* **102**: 14469–14474.

Yang XJ, Seto E. 2008. The Rpd3/Hda1 family of lysine deacetylases: from bacteria and yeast to mice and men. *Nature Reviews Molecular Cell Biology* **9**: 206–218.

Yoo SK, Chung KS, Kim J, Lee JH, Hong SM, Yoo SJ, Yoo SY, Lee JS, Ahn JH. 2005. CONSTANS activates *SUPPRESSOR OF OVEREXPRESSION OF CONSTANS 1* through *FLOWERING LOCUS T* to promote flowering in Arabidopsis. *Plant Physiology* **139**: 770–778.

Yoo SK, Wu X, Lee JS, Ahn JH. 2011. *AGAMOUS-LIKE 6* is a floral promoter that negatively regulates the *FLC/MAF* clade genes and positively regulates *FT* in Arabidopsis. *Plant Journal* **65**: 62–76.

Yu H, Xu Y, Tan EL, Kumar PP. 2002. AGAMOUS-LIKE 24, a dosage-dependent mediator of the flowering signals. *Proceedings of the National Academy of Sciences, USA* **99**: 16336–16341.

Yu CW, Liu X, Luo M, Chen C, Lin X, Tian G, Lu Q, Cui Y, Wu K. 2011. HISTONE DEACETYLASE6 interacts with FLOWERING LOCUS D and regulates flowering in Arabidopsis. *Plant Physiology* **156**: 172–184.

Zhou C, Zhang L, Duan J, Miki B, Wu K. 2005. *HISTONE DEACETYLASE 19* is involved in jasmonic acid and ethylene signaling of pathogen response in Arabidopsis. *Plant Cell* **17**: 1196–1204.

Supporting Information

Additional supporting information may be found in the online version of this article.

Fig. S1 Sequence comparison between *Arabidopsis thaliana* class I HDAC proteins.

Fig. S2 Effect of the *Arabidopsis thaliana hda9-1* mutation on silique and petiole lengths.

Fig. S3 Predicted spatial expression profile of *Arabidopsis thaliana HDA9*.

Fig. S4 Complementation of the early-flowering phenotype of *Arabidopsis thaliana hda9-1* by *HDA9:HA*.

Fig. S5 T-DNA insertion mutants for *Arabidopsis thaliana MAF4* and *MAF5*.

Fig. S6 Expression of genes encoding *FT* regulators and SPL-family transcription factors in *Arabidopsis thaliana hda9-1*.

Fig. S7 *SOC1* is not a direct target of *Arabidopsis thaliana* HDA9.

Table S1 Oligonucleotides used for genotyping

Table S2 Oligonucleotides used for *HDA9g*, *HDA9:GUS*, and *HDA9:HA* constructs

Table S3 Oligonucleotides used for RT-PCR analysis

Table S4 Oligonucleotides used for RT-qPCR analyses

Table S5 Oligonucleotides used for ChIP assays

Please note: Wiley Blackwell are not responsible for the content or functionality of any supporting information supplied by the authors. Any queries (other than missing material) should be directed to the *New Phytologist* Central Office.